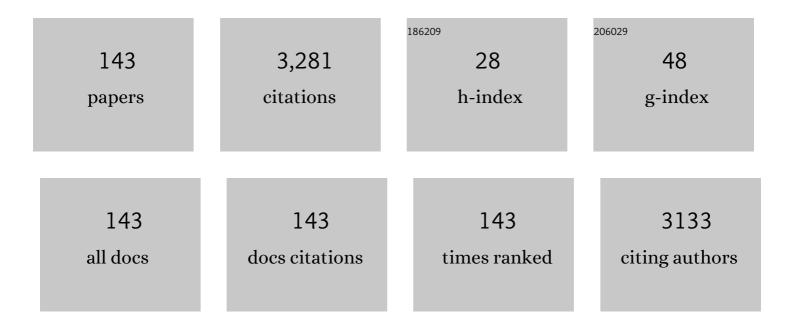
List of Publications by Year in descending order

Source: https://exaly.com/author-pdf/4449397/publications.pdf Version: 2024-02-01



DENCMAN CHEN

#	Article	lF	CITATIONS
1	Interfacial Residual Stress Relaxation in Perovskite Solar Cells with Improved Stability. Advanced Materials, 2019, 31, e1904408.	11.1	259
2	Edgeâ€ŧo dge Assembled Graphene Oxide Aerogels with Outstanding Mechanical Performance and Superhigh Chemical Activity. Small, 2013, 9, 1397-1404.	5.2	182
3	Evaluation of the quality of a speckle pattern in the digital image correlation method by mean subset fluctuation. Optics and Laser Technology, 2011, 43, 9-13.	2.2	137
4	Recent progress in carbonyl-based organic polymers as promising electrode materials for lithium-ion batteries (LIBs). Journal of Materials Chemistry A, 2020, 8, 11906-11922.	5.2	134
5	Characterization of the condensed carbon in detonation soot. Carbon, 2003, 41, 2093-2099.	5.4	107
6	One-step solution combustion synthesis of CuO/Cu2O/C anode for long cycle life Li-ion batteries. Carbon, 2019, 142, 51-59.	5.4	79
7	Residual stress in thermal spray coatings measured by curvature based on 3D digital image correlation technique. Surface and Coatings Technology, 2011, 206, 1396-1402.	2.2	68
8	Microstructure, deformation and failure of polymer bonded explosives. Journal of Materials Science, 2007, 42, 5272-5280.	1.7	64
9	Deformation and failure of polymer bonded explosives under diametric compression test. Polymer Testing, 2006, 25, 333-341.	2.3	59
10	Experimental study on the micromechanical behavior of a PBX simulant using SEM and digital image correlation method. Optics and Lasers in Engineering, 2011, 49, 366-370.	2.0	58
11	Self-Assembling VO ₂ Nanonet with High Switching Performance at Wafer-Scale. Chemistry of Materials, 2015, 27, 7419-7424.	3.2	58
12	Evolution of Structural and Electrical Properties of Oxygen-Deficient VO ₂ under Low Temperature Heating Process. ACS Applied Materials & Interfaces, 2017, 9, 27135-27141.	4.0	52
13	Molecular Hinges Stabilize Formamidiniumâ€Based Perovskite Solar Cells with Compressive Strain. Advanced Functional Materials, 2022, 32, .	7.8	50
14	Numerical and Experimental Studies on the Explosive Welding of Tungsten Foil to Copper. Materials, 2017, 10, 984.	1.3	48
15	Microstructure characterization and tensile shear failure mechanism of the bonding interface of explosively welded titanium-steel composite. Materials Science & Engineering A: Structural Materials: Properties, Microstructure and Processing, 2021, 820, 141559.	2.6	47
16	Modeling ignition prediction of HMX-based polymer bonded explosives under low velocity impact. Mechanics of Materials, 2018, 124, 106-117.	1.7	43
17	Investigation on the Explosive Welding of 1100 Aluminum Alloy and AZ31 Magnesium Alloy. Journal of Materials Engineering and Performance, 2016, 25, 2635-2641.	1.2	42
18	Monitoring micro-structural evolution during aluminum sintering and understanding the sintering mechanism of aluminum nanoparticles: A molecular dynamics study. Journal of Materials Science and Technology, 2020, 57, 92-100.	5.6	42

#	Article	IF	CITATIONS
19	High-strain-rate plastic deformation and fracture behaviour of Ti-5Al-5Mo-5V-1Cr-1Fe titanium alloy at room temperature. Mechanics of Materials, 2018, 116, 3-10.	1.7	39
20	Cross-Sectional Residual Stresses in Thermal Spray Coatings Measured by Moiré Interferometry and Nanoindentation Technique. Journal of Thermal Spray Technology, 2012, 21, 810-817.	1.6	36
21	Dynamic shear deformation and failure of Ti-5Al-5Mo-5V-1Cr-1Fe titanium alloy. Materials Science & Engineering A: Structural Materials: Properties, Microstructure and Processing, 2017, 694, 41-47.	2.6	35
22	Effect of microstructure on mechanical properties of titanium-steel explosive welding interface. Materials Science & Engineering A: Structural Materials: Properties, Microstructure and Processing, 2022, 830, 142260.	2.6	35
23	Fabrication of W–Cu composite by shock consolidation of Cu-coated W powders. Journal of Alloys and Compounds, 2016, 657, 215-223.	2.8	34
24	Fabrication and characterization of the Ni–Al energetic structural material with high energy density and mechanical properties. Journal of Alloys and Compounds, 2020, 832, 154894.	2.8	33
25	Hydrothermal growth of VO2 nanoplate thermochromic films on glass with high visible transmittance. Scientific Reports, 2016, 6, 27898.	1.6	32
26	Nonâ€Shock Ignition Probability of Octahydroâ€1,3,5,7â€Tetranitroâ€Tetrazocineâ€Based Polymer Bonded Explosives Based on Microcrack Stochastic Distribution. Propellants, Explosives, Pyrotechnics, 2020, 45, 568-580.	1.0	32
27	Joining AlCoCrFeNi high entropy alloys and Al-6061 by explosive welding method. Vacuum, 2020, 174, 109221.	1.6	32
28	Enhanced synthesis method of graphene oxide. Nanoscale Advances, 2021, 3, 223-230.	2.2	30
29	The combustion behavior of boron particles by using molecular perovskite energetic materials as high-energy oxidants. Combustion and Flame, 2022, 241, 112118.	2.8	30
30	Buckling modes of polymer membranes restricted by metal wires. Soft Matter, 2011, 7, 2888.	1.2	29
31	Shock-wave synthesis of multilayer graphene and nitrogen-doped graphene materials from carbonate. Carbon, 2015, 94, 928-935.	5.4	29
32	Fabrication of visible-light-driven Ag/TiO2 heterojunction composites induced by shock wave. Journal of Alloys and Compounds, 2016, 679, 463-469.	2.8	29
33	Preparation of graphene by electrical explosion of graphite sticks. Nanoscale, 2017, 9, 10639-10646.	2.8	29
34	Ignition criterion and safety prediction of explosives under low velocity impact. Journal of Applied Physics, 2013, 114, .	1.1	28
35	Effects of microstructure on the dynamic properties of TA15 titanium alloy. Mechanics of Materials, 2019, 137, 103121.	1.7	28
36	Fabrication technique of micro/nano-scale speckle patterns with focused ion beam. Science China: Physics, Mechanics and Astronomy, 2012, 55, 1037-1044.	2.0	27

#	Article	IF	CITATIONS
37	Experimental and Numerical Study on Microstructure and Mechanical Properties of Ti-6Al-4V/Al-1060 Explosive Welding. Metals, 2019, 9, 1189.	1.0	27
38	The role of tension–compression asymmetrical microcrack evolution in the ignition of polymer-bonded explosives under low-velocity impact. Journal of Applied Physics, 2021, 129, .	1.1	27
39	Detection and characterization of long-pulse low-velocity impact damage in plastic bonded explosives. International Journal of Impact Engineering, 2005, 31, 497-508.	2.4	25
40	Characterization of fine-grained W–10wt.% Cu composite fabricated by hot-shock consolidation. International Journal of Refractory Metals and Hard Materials, 2015, 52, 137-142.	1.7	25
41	A corrugated gradient mechanical metamaterial: Lightweight, tunable auxeticity and enhanced specific energy absorption. Thin-Walled Structures, 2022, 176, 109355.	2.7	25
42	Controlled Ag-TiO 2 heterojunction obtained by combining physical vapor deposition and bifunctional surface modifiers. Journal of Physics and Chemistry of Solids, 2018, 119, 147-156.	1.9	24
43	Comprehensive simulations of rock fracturing with pre-existing cracks by the numerical manifold method. Acta Geotechnica, 2022, 17, 857-876.	2.9	24
44	Solvent-less method for efficient photocatalytic α-Fe2O3 nanoparticles using macromolecular polymeric precursors. New Journal of Chemistry, 2016, 40, 6768-6776.	1.4	23
45	One Step Preparation of Fe–FeO–Graphene Nanocomposite through Pulsed Wire Discharge. Crystals, 2018, 8, 104.	1.0	23
46	High strain rate deformation of explosion-welded Ti6Al4V/pure titanium. Defence Technology, 2020, 16, 678-688.	2.1	23
47	Recent strategies to improve moisture stability in metal halide perovskites materials and devices. Journal of Energy Chemistry, 2022, 65, 219-235.	7.1	23
48	Observation of damage evolution in polymer bonded explosives using acoustic emission and digital image correlation. Polymer Testing, 2011, 30, 861-866.	2.3	22
49	Simulations of meso-scale deformation and damage of polymer bonded explosives by the numerical manifold method. Engineering Analysis With Boundary Elements, 2018, 96, 123-137.	2.0	22
50	Nitrogen-doped titania photocatalysts induced by shock wave. Materials Research Bulletin, 2009, 44, 1842-1845.	2.7	21
51	One-step detonation-assisted synthesis of Fe ₃ O ₄ -Fe@BCNT composite towards high performance lithium-ion batteries. Nanoscale, 2017, 9, 14376-14384.	2.8	21
52	Effect of microstructure on the mechanical properties of Ti–5Al–5Mo–5V–1Cr–1Fe alloy. Materials Science & Engineering A: Structural Materials: Properties, Microstructure and Processing, 2020, 773, 138728.	2.6	21
53	Investigation on the interfacial microstructure and mechanical properties of the W-Cu joints fabricated by hot explosive welding. Journal of Materials Processing Technology, 2022, 300, 117400.	3.1	20
54	Welding Window: Comparison of Deribas' and Wittman's Approaches and SPH Simulation Results. Metals, 2019, 9, 1323.	1.0	19

#	Article	IF	CITATIONS
55	Quasi-static in-plane compression of zig-zag folded metamaterials at large plastic strains. Thin-Walled Structures, 2021, 159, 107285.	2.7	19
56	Dynamic mechanical contact behaviors and sintering mechanism of Al nanoparticles subjected to high-speed impact. Materials Chemistry and Physics, 2021, 273, 125111.	2.0	19
57	Comparative study of the fracture toughness determination of a polymer-bonded explosive simulant. Engineering Fracture Mechanics, 2011, 78, 2991-2997.	2.0	18
58	Quasi-static tensile deformation and fracture behavior of a highly particle-filled composite using digital image correlation method. Theoretical and Applied Mechanics Letters, 2011, 1, 051002.	1.3	18
59	Reaction synthesis of TiSi2 and Ti5Si3 by ball-milling and shock loading and their photocatalytic activities. Journal of Alloys and Compounds, 2013, 555, 375-380.	2.8	18
60	Fabrication of Nanocrystalline AlCoCrFeNi High Entropy Alloy through Shock Consolidation and Mechanical Alloying. Entropy, 2019, 21, 880.	1.1	18
61	Symmetric Confined Growth of Superstructured Vanadium Dioxide Nanonet with a Regular Geometrical Pattern by a Solution Approach. Crystal Growth and Design, 2017, 17, 5838-5844.	1.4	17
62	Shear localization and recrystallization in high strain rate deformation in Ti-5Al-5Mo-5V-1Cr-1Fe alloy. Materials Letters, 2018, 232, 142-145.	1.3	17
63	Fabrication and characterization of the Mo/cu bimetal with thick Mo layer and high interfacial strength. International Journal of Refractory Metals and Hard Materials, 2021, 94, 105383.	1.7	17
64	Shock induced conversion of carbon dioxide to few layer graphene. Carbon, 2017, 115, 471-476.	5.4	17
65	Fabrication and characterization of pure tungsten using the hot-shock consolidation. International Journal of Refractory Metals and Hard Materials, 2014, 42, 215-220.	1.7	16
66	Stabilizing Metastable Polymorphs of Metal–Organic Frameworks via Encapsulation of Graphene Oxide and Mechanistic Studies. ACS Applied Materials & Interfaces, 2018, 10, 32828-32837.	4.0	16
67	Dynamic Shear Deformation and Failure of Ti-6Al-4V and Ti-5Al-5Mo-5V-1Cr-1Fe Alloys. Materials, 2018, 11, 76.	1.3	16
68	Investigation on Explosive Welding of Zr53Cu35Al12 Bulk Metallic Glass with Crystalline Copper. Journal of Materials Engineering and Performance, 2018, 27, 2932-2937.	1.2	16
69	Dynamic behavior and adiabatic shearing formation of the commercially pure titanium with explosion-induced gradient microstructure. Materials Science & Engineering A: Structural Materials: Properties, Microstructure and Processing, 2022, 833, 142340.	2.6	16
70	Synthesis of N-doped TiO ₂ with Different Nitrogen Concentrations by Mild Hydrothermal Method. Materials and Manufacturing Processes, 2014, 29, 1162-1167.	2.7	15
71	The effect of heating rate on the sintering of aluminum nanospheres. Physical Chemistry Chemical Physics, 2021, 23, 11684-11697.	1.3	15
72	Dynamic forced shear characteristics of Ti-6Al-4V alloy using flat hat-shaped specimen. Engineering Fracture Mechanics, 2020, 238, 107286.	2.0	14

#	Article	IF	CITATIONS
73	Comparative experimental study of the dynamic properties and adiabatic shear susceptibility of titanium alloys. European Journal of Mechanics, A/Solids, 2021, 85, 104137.	2.1	14
74	Meso-scale failure simulation of polymer bonded explosive with initial defects by the numerical manifold method. Computational Materials Science, 2020, 173, 109425.	1.4	13
75	Modelling Microstructural Deformation and the Failure Process of Plastic Bonded Explosives Using the Cohesive Zone Model. Materials, 2019, 12, 3661.	1.3	12
76	Effects of microstructure on mechanical and energy release properties of Ni–Al energetic structural materials. Materials Science & Engineering A: Structural Materials: Properties, Microstructure and Processing, 2022, 849, 143332.	2.6	12
77	One-pot hydrothermal synthesis of flower-like MnO2 nanostructure with rich oxygen vacancy for catalysis thermal-induced pyrolysis of energetic molecular perovskite. Vacuum, 2022, 203, 111234.	1.6	12
78	Study on the mechanical behavior of adhesive interface by digital image correlation. Science China: Physics, Mechanics and Astronomy, 2011, 54, 574-580.	2.0	11
79	Formation of bonding interface in explosive welding—a molecular dynamics approach. Journal of Physics Condensed Matter, 2019, 31, 415403.	0.7	11
80	Shock-induced large-depth gradient microstructure in commercial pure titanium subjected to explosive hardening. Materials and Design, 2022, 213, 110309.	3.3	11
81	Scalable Conversion of CO2 to N-Doped Carbon Foam for Efficient Oxygen Reduction Reaction and Lithium Storage. ACS Sustainable Chemistry and Engineering, 2018, 6, 3358-3366.	3.2	10
82	CO2 Conversion into N-Doped Carbon Nanomesh Sheets. ACS Applied Nano Materials, 2019, 2, 2991-2998.	2.4	10
83	Quasi-static compression properties of graphene aerogel. Diamond and Related Materials, 2021, 111, 108225.	1.8	10
84	The influence of the drying method on the microstructure and the compression behavior of graphene aerogel. Diamond and Related Materials, 2022, 121, 108772.	1.8	10
85	Microstructure and mechanical properties of the bonding interface of explosively welded TA2/Q235 composite under dynamic shear loading. International Journal of Mechanical Sciences, 2022, 225, 107362.	3.6	10
86	Effect of strain rate and temperature on deformation and recrystallization behaviour of BCC structure AlCoCrFeNi high entropy alloy. Intermetallics, 2022, 147, 107601.	1.8	10
87	Impact energy absorption behavior of graphene aerogels prepared by different drying methods. Materials and Design, 2022, 221, 110912.	3.3	10
88	Enhanced visible-light absorption of nitrogen-doped titania induced by shock wave. Materials Letters, 2011, 65, 685-687.	1.3	9
89	Effects of Specimen Size on Impact-Induced Reaction of High Explosives. Combustion Science and Technology, 2013, 185, 1227-1240.	1.2	9
90	Shock-induced phase transition of g-C3N4 to a new C3N4 phase. Journal of Applied Physics, 2019, 126, .	1.1	9

#	Article	IF	CITATIONS
91	Synthesis of nano titanium oxide with controlled oxygen content using pulsed discharge in water. Advanced Powder Technology, 2020, 31, 986-992.	2.0	9
92	Topography-driven delamination of thin patch adhered to wrinkling surface. International Journal of Mechanical Sciences, 2020, 178, 105622.	3.6	9
93	Simulation of force chains and particle breakage of granular material by numerical manifold method. Powder Technology, 2021, 390, 464-472.	2.1	9
94	One-step combustion synthesis of carbon-coated NiO/Ni composites for lithium and sodium storage. Journal of Alloys and Compounds, 2021, 884, 160927. Iar dynamics simulations of complimath	2.8	9
95	xmins:mml="nttp://www.w3.org/1998/Math/MathML"> <mml:mrow><mml:mi mathvariant="normal">C<mml:msub><mml:mi mathvariant="normal">u<mml:mn>46</mml:mn></mml:mi </mml:msub><mml:mi mathvariant="normal">Z<mml:msub><mml:mi< td=""><td>1.1</td><td>8</td></mml:mi<></mml:msub></mml:mi </mml:mi </mml:mrow>	1.1	8
96	High-Efficiency Production of Large-Size Few-Layer Graphene Platelets via Pulsed Discharge of Graphite Strips. Nanomaterials, 2019, 9, 1785.	1.9	8
97	Hierarchical Surface Patterns via Global Wrinkling on Curved Substrate for Fluid Drag Control. Advanced Materials Interfaces, 2021, 8, .	1.9	8
98	Atomistic simulation on the formation mechanism of bonding interface in explosive welding. Journal of Applied Physics, 2022, 131, .	1.1	8
99	Mechanical behavior of PBX with different HMX crystal size during die pressing: Experimental study and DEM simulation. Composites Science and Technology, 2022, 222, 109378.	3.8	8
100	Response of Graded Miura-Ori Metamaterials to Quasi-Static and Dynamic In-Plane Compression. Journal of Aerospace Engineering, 2022, 35, .	0.8	8
101	Chemical reaction of Ni/Al interface associated with perturbation growth under shock compression. Physics of Fluids, 2022, 34, .	1.6	8
102	Optical characterization of nanocarbon phases in detonation soot and shocked graphite. Diamond and Related Materials, 2006, 15, 1400-1404.	1.8	7
103	Preparation of Few-Layer Graphene by Pulsed Discharge in Graphite Micro-Flake Suspension. Crystals, 2019, 9, 150.	1.0	7
104	Meso-structure construction and effective modulus simulation of PBXs. Journal of Energetic Materials, 2020, 38, 261-282.	1.0	7
105	Dynamic contact behaviours involving crystalline diamond nanospheres. European Journal of Mechanics, A/Solids, 2020, 80, 103896.	2.1	7
106	Microstructural characterization of pressure-induced cracking in melamine/F2311 composites and crack-healing behavior via thermal-pressure aging treatment. Materials and Design, 2020, 189, 108538.	3.3	7
107	Shock-induced consolidation of tungsten nanoparticles—A molecular dynamics approach. Journal of Applied Physics, 2020, 127, .	1.1	7
108	Dynamic mechanical contact behaviours of amorphous nanoparticles subjected to high-speed impact. Powder Technology, 2020, 364, 689-697.	2.1	7

#	Article	IF	CITATIONS
109	One-step synthesis of FeO(OH) nanoparticles by electric explosion of iron wire underwater. Defence Technology, 2022, 18, 133-139.	2.1	7
110	Predicting the mechanical behaviour of highly particle-filled polymer composites using the nonlinear finite element method. Composite Structures, 2022, 286, 115275.	3.1	7
111	Effect of particle morphology on mechanical behaviour of highly particle-filled composites. International Journal of Mechanical Sciences, 2022, 227, 107446.	3.6	7
112	Macro-Micro Mechanical Behavior of a Highly-Particle-Filled Composite Using Digital Image Correlation Method. , 0, , .		6
113	Measurement of dynamic fracture toughness and failure behavior for explosive mock materials. Frontiers of Mechanical Engineering, 2011, 6, 292.	2.5	6
114	A New S-Shape Specimen for Studying the Dynamic Shear Behavior of Metals. Metals, 2019, 9, 838.	1.0	6
115	Graphene Formation through Pulsed Wire Discharge of Graphite Strips in Water: Exfoliation Mechanism. Nanomaterials, 2021, 11, 1223.	1.9	6
116	Mechanical behavior simulation of particulate-filled composite at meso-scale by numerical manifold method. International Journal of Mechanical Sciences, 2022, 213, 106846.	3.6	6
117	Shock induced gradient microstructure with hierarchical nanotwins to enhance mechanical properties of Ti6Al4V alloy. Journal of Materials Processing Technology, 2022, 307, 117693.	3.1	6
118	Study on dynamic fracture and mechanical properties of a PBX simulant by using dic and SHPB method. , 2012, , .		5
119	Fabrication of tungsten-copper composites by hot-shock consolidation. , 2012, , .		5
120	Detonation Synthesis of Carbon-Encapsulated Magnetic Nanoparticles. Fullerenes Nanotubes and Carbon Nanostructures, 2015, 23, 605-611.	1.0	5
121	Effect of Continuous Damage Accumulation on Ignition of HMXâ€Based Polymer Bonded Explosives under Lowâ€Velocity Impact. Propellants, Explosives, Pyrotechnics, 2020, 45, 1908-1919.	1.0	5
122	Dynamic mesoscale cracking modeling of energetic composite materials in Hopkinson bar test. Composite Structures, 2022, 281, 114989.	3.1	5
123	Dynamic penetration behaviors of single/multi-layer graphene using nanoprojectile under hypervelocity impact. Scientific Reports, 2022, 12, 7440.	1.6	5
124	Detonation-assisted self-assembly synthesis of carbon onions using organics with long carbon chain. Fullerenes Nanotubes and Carbon Nanostructures, 2017, 25, 163-169.	1.0	4
125	A molecular dynamics study on the chemical reaction of Ni/Al reactive intermetallics. Journal of Applied Physics, 2020, 128, 185901.	1.1	4
126	Research on the Ignition Height and Reaction Flame Temperature of PTFE/Al/Si/CuO with Different Mass Ratios of PTFE/Si. Materials, 2021, 14, 3464.	1.3	4

#	Article	IF	CITATIONS
127	Tensile behavior of the titanium-steel explosive welded interface under quasi-static and high-strain rate loading. International Journal of Solids and Structures, 2022, 254-255, 111870.	1.3	4
128	Characterization of Ta-Ni-Al energetic structural material fabricated by explosive consolidation. Journal of Alloys and Compounds, 2022, 924, 166191.	2.8	4
129	Specimen size effect of explosive sensitivity under low velocity impact. Journal of Physics: Conference Series, 2014, 500, 052026.	0.3	3
130	Local shear dominance in equation of state of metallic glass under hydrostatic pressure. Journal of Applied Physics, 2018, 124, 165901.	1.1	3
131	Absence of 2.5 power law for fractal packing in metallic glasses. Journal of Physics Condensed Matter, 2018, 30, 255402.	0.7	3
132	Formation of nanodiamond by pulsed discharge of carbon fiber wires. Applied Physics Letters, 2020, 117, .	1.5	3
133	Shock Consolidation of Ni/Al Nanoparticles: A Molecular Dynamics Simulation. Journal of Materials Engineering and Performance, 0, , 1.	1.2	3
134	Formation of black phosphorus quantum dots via shock-induced phase transformation. Applied Physics Letters, 2022, 120, .	1.5	3
135	Ti-Si photocatalyst for producing hydrogen synthesized by shock wave. , 2012, , .		2
136	Comparative Study of the Dynamic Fracture Toughness Determination of Brittle Materials Using the Kolsky-Hopkinson Bar Machine. , 2018, , 143-156.		1
137	Microstructural Evolution in High-Strain-Rate Deformation of Ti-5Al-5Mo-5V-1Cr-1Fe Alloy. Materials, 2018, 11, 839.	1.3	1
138	CO2 Conversion into N-Doped Porous Carbon-Encapsulated NiO/Ni Composite Nanomaterials as Outstanding Anode Material of Li Battery. Nanomaterials, 2020, 10, 1502.	1.9	1
139	Modeling of Impact Energy Release of PTFE/Al Reactive Material. Applied Sciences (Switzerland), 2021, 11, 8910.	1.3	1
140	Shock synthesis of nanocrystalline La2Ti2O7 powder. Journal of Applied Physics, 2021, 130, 125903.	1.1	1
141	Measurement of the Dynamic Fracture Toughness of Alumina Ceramic. Conference Proceedings of the Society for Experimental Mechanics, 2016, , 33-38.	0.3	1
142	Gram-Scale Preparation of Black Phosphorus Nanosheets via Shock-Induced Phase Transformation. Journal of Materials Chemistry C, 0, , .	2.7	1
143	Dynamic Brazilian Test Using the Kolsky-Hopkinson Bar Machine. , 2018, , 121-141.		0